Available online at www.sciencedirect.com

ScienceDirect

Journal of Photochemistry and Photobiology A: Chemistry 188 (2007) 409–418

Journal of Photochemistry and Photobiology A:Chemistry

www.elsevier.com/locate/jphotochem

Comparative study of the UV and UV/VUV-induced photolysis of phenol in aqueous solution

Tünde Alapi, András Dombi *

Department of Inorganic and Analytical Chemistry, University of Szeged, P.O. Box 440, Szeged H-6701, Hungary

Received 30 October 2006; received in revised form 2 January 2007; accepted 3 January 2007
Available online 7 January 2007

Abstract

The UV (254 nm) and UV/VUV (254/185 nm) photolysis of phenol and the distribution of the products in solutions saturated with oxygen or nitrogen were investigated and compared. The initial rate of degradation of phenol in UV/VUV-irradiated solutions exceeded that determined in UV-irradiated solutions, but the difference decreased dramatically with increase of the initial phenol concentration. The effects of methanol as $HO^•$ scavenger demonstrated that the relative contribution of the $HO^•$-based reactions to the decomposition of phenol in UV/VUV-irradiated solutions decreased strongly with increase of the initial phenol concentration. The same aromatic (1,2- and 1,4-dihydroxybenzene) and aliphatic (maleic, malic, tartaric and oxalic acids) intermediates were detected in UV- and UV/VUV-irradiated solutions saturated with oxygen. The decompositions of 1,2- and 1,4-dihydroxybenzene, 1,4-benzoquinone and oxalic acid were also investigated both in UV/VUV- and in UV-irradiated solutions.

Keywords: 254 nm; 185 nm; Hydroxyl radical; Phenoxyl radical; Phenol

1. Introduction

The potential of advanced oxidation processes to remove both organic and inorganic compounds from water or air is currently being intensively studied. These processes include direct ultraviolet (UV) and vacuum-ultraviolet (VUV) photolysis, which are promising methods for the production of drinking water or ultrapure water without the addition of other reagents. These methods can be successfully applied to remove aromatic pollutants such as phenols. It should be noted, however that UV irradiation alone cannot be used as an effective procedure for the total mineralization of organics, whereas it is quite efficient for water disinfection [1]. At the same time, the $HO^•$ generated from water by VUV light is one of the most reactive and nonselective species, which can react at high rates with almost any organic substances. Thus, a number of technologies are based on the $HO^•$-initiated reactions for the complete removal of organic pollutants from aqueous solutions.

The commercially available low-pressure mercury vapour lamp is a light source widely applied in water purification and disinfection technologies. This light source has its main output at 254 nm, with a small amount (6% of the total intensity of irradiation) at 185 nm [2]. The generally low quantum yield and the relatively small molar absorptivity of the target compounds at 254 nm are factors that limit the efficiency, and therefore the applicability of direct photolysis process in water remediation [3]. The extinction coefficient for phenol at 254 nm is $516\ \mathrm{mol^{-1}\ dm^3\ cm^{-1}}$ and the quantum yield of phenol photooxidation in aerated solutions has been found to vary in the interval 0.12–0.02 at pH 1.6–13.2, with a minimum value at pH 11.1 [4].

The excitation of phenol leads to the formation of its first excited singlet state (1), which can decay by fluorescence (298 nm) (2) [5,6], radiationless internal conversion to the ground state (3), intersystem crossing to the triplet state (4) [6], chemical dissociation into phenoxyl radical ($ArO^•$) and $H^•$ (5) [7,8], photoionization (6) [9,10] and product formation (7). Naturally, the relative contributions of these reactions to the decay of the excited state depend strongly on the experimental parameters:

$$\mathrm{phenol} + h\nu \rightarrow {}^1\mathrm{phenol} \tag{1}$$

$$^1\mathrm{phenol} \rightarrow \mathrm{phenol} + h\nu' \tag{2}$$

$$^1\mathrm{phenol} \rightarrow \mathrm{phenol} \tag{3}$$

---

* Corresponding author. Tel.: +36 62 544 335; fax: +36 62 420 505.
E-mail address: dombia@chem.u-szeged.hu (A. Dombi).

1010-6030/$ – see front matter © 2007 Elsevier B.V. All rights reserved.
doi:10.1016/j.jphotochem.2007.01.002

$$^{1}\text{phenol} \rightarrow {}^{3}\text{phenol} \quad (4)$$

$$^{1}\text{phenol} \rightarrow ({}^{3}\text{phenol}) \rightarrow \text{ArO}^{\bullet} + {}^{\bullet}\text{H} \quad (5)$$

$$\begin{aligned} &^{1}\text{phenol} \rightarrow {}^{3}\text{phenol} \xrightarrow{h\nu} \text{ArOH}^{\bullet+} + \text{e}_{\text{aq}}^{-} \\ &\xrightarrow{\text{H}_2\text{O/H}^+} \text{ArO}^{\bullet} + \text{H}^{+} + \text{e}_{\text{aq}}^{-} \rightarrow \text{ArO}^{\bullet} + {}^{\bullet}\text{H} \quad (6) \end{aligned}$$

$$^{1}\text{phenol} \rightarrow \text{products} \quad (7)$$

$$^{3}\text{phenol} + \text{O}_2 \rightarrow \text{phenol} + {}^{1}\text{O}_2 \quad (8)$$

$$^{3}\text{phenol} + \text{O}_2 \rightarrow \text{ArO}^{\bullet+} + \text{O}_2{}^{\bullet-} \quad (9)$$

The quantum yield of $\text{H}^{\bullet}$ formation (5) and photoionization (6) depend on the nature of the solvent, on the pH of the solution and on the wavelength of excitation [8]. In neutral or acidic aqueous solutions (pH 7–2) excitation to singlet-state phenol at 266 nm leads primarily to photoionization. Besides this, $\text{H}^{\bullet}$ formation (5) is a very minor path likely because homolytic cleavage of the O–H bond of phenol is suppressed by H-bonding with water molecules. Most phenoxyl radical cations are generated via a biphotonic process [7,11] in neutral and acidic solutions if a second photon is absorbed by the triplet state of the phenol molecule. The radical cation formed is not stable in aqueous solutions, it rapidly deprotonation yielding a phenoxyl radical [12]. Besides decaying to the ground state by fluorescence and photoionization, the triplet-excited state of phenol can be quenched by oxygen. A fraction of this reaction can lead to the formation of singlet oxygen ($^{1}\text{O}_2$) (8) or $\text{O}_2{}^{\bullet-}$ (9).

VUV light generates $\text{HO}^{\bullet}$ from water. In water, homolysis to $\text{HO}^{\bullet}$ and $\text{H}^{\bullet}$ takes place with a quantum yield ($\Phi_{\text{HO}^{\bullet}}$) at 185 nm of 0.33 [13]. The penetration depth for VUV light in water is very short, about 0.1 mm. During the degradation of aromatic compounds, the first step is generally nucleophilic addition of $\text{HO}^{\bullet}$ to the aromatic ring [13].

Dissolved oxygen strongly influences the quality and quantity of the reactive species in irradiated aqueous solutions. This can open up the pathway for the formation of peroxyl-type organic radicals ($\text{R}^{\bullet} + \text{O}_2 \rightarrow \text{ROO}^{\bullet}$), $\text{HO}_2{}^{\bullet}$ ($\text{H}^{\bullet} + \text{O}_2 \rightarrow \text{HO}_2{}^{\bullet}$, $k = 1.4 \times 10^{10}\ \text{dm}^3\ \text{mol}^{-1}\ \text{s}^{-1}$ [14]), or $\text{O}_2{}^{\bullet-}$ ($\text{O}_2 + \text{e}^- \rightarrow \text{O}_2{}^{\bullet-}$, $k = 1.9 \times 10^{10}\ \text{dm}^3\ \text{mol}^{-1}\ \text{s}^{-1}$ [15]). $\text{HO}_2{}^{\bullet}$ is in equilibrium with its conjugated base, $\text{O}_2{}^{\bullet-}$; $\text{p}K = 4.8$ [15]. The further transformation of the organic peroxyl-type radicals involves $\text{HO}_2{}^{\bullet}$ and $\text{O}_2{}^{\bullet-}$ elimination [16]. Thus, in oxygen-containing aqueous solution, the direct photooxidation of organics has a quite complex chemism.

In the present work, the direct photolysis of phenol in aqueous solutions was investigated by using low-pressure mercury vapour lamps immersed in the irradiated solution. The aims were to compare the efficiencies of two different low-pressure mercury lamps in the decomposition of phenol and its intermediates in solutions saturated with oxygen or in oxygen-free solutions, and to investigate the relative contributions of $\text{HO}^{\bullet}$-based reactions and the direct photolysis-initiated decompositions of phenol in UV/VUV-irradiated solutions.

2. Materials and methods

Both of the low-pressure mercury vapour lamps applied were made by LightTech (Hungary, Dunakeszi) and had identical geometry (307 mm long and a 20.5 mm external diameter sleeve) and electric parameters (15 W electric and 4.0 W UV output). The lamp emitting at 254 nm (GCL307T5VH/CELL) was covered with a commercial quartz sleeve (UV lamp). The lamp emitting at both 254 and 185 nm (GCL307T5/CELL) was covered with a Suprasil sleeve (UV/VUV lamp). The emitted photon flux of the light sources was measured by potassium ferrioxalate actinometry [17]. The photon flux of the 254 nm component of both lamps was independent of the material of the sleeve, and was found to be $3.45 \pm 0.09 \times 10^{-5}\ \text{mol}_{\text{photon}}\ \text{s}^{-1}$. The actinometric measurements were carried out by using the same volume as that of the irradiated phenol solutions in the reactor. The emission spectra of the low-pressure mercury lamps, measured with a T3000-RT-UV-VIS photometer in the wavelength range 200–890 nm, were found to be identical for the two lamps. The photon flux of the 185 nm component of the light emitted by UV/VUV lamp was estimated to be $2.1 \times 10^{-6}\ \text{mol}_{\text{photon}}\ \text{s}^{-1}$ according to the data given by LightTech.

The decomposition and mineralization of phenol were investigated under four different conditions: irradiation with UV or UV/VUV light, in solutions saturated with oxygen or nitrogen. The initial concentrations of phenol were adjusted in the range $(0.1\text{–}2.0) \times 10^{-3}\ \text{mol dm}^{-3}$.

The effects of methanol as $\text{HO}^{\bullet}$ scavenger were also investigated. Phenol of analytical grade from Sigma was dissolved in ultrapure water without any buffering. Methanol was of HPLC grade from Scharlau. In each experiment ultrapure water obtained from a Millipore purifier (Milli-Q) was applied.

The experimental apparatus is shown in Fig. 1. The low-pressure mercury lamp (3) was centred in the water-cooled,

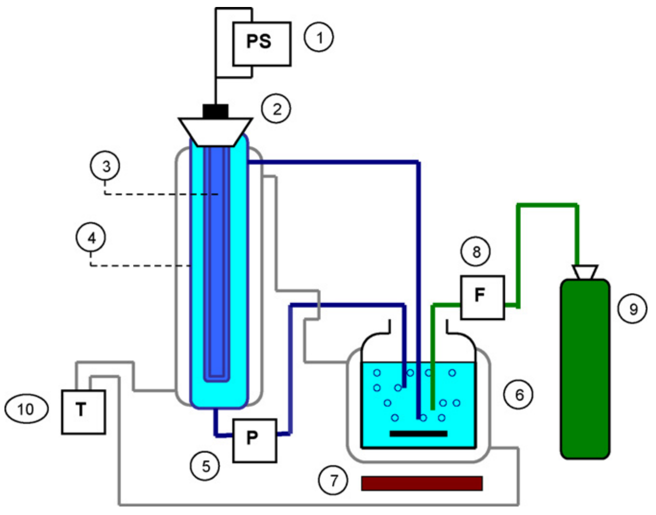

Fig. 1. Experimental apparatus: (1) power supply; (2) Teflon packing ring; (3) UV or UV/VUV lamp; (4) reactor; (5) pump; (6) reservoir; (7) magnetic stirrer; (8) flow meter; (9) oxygen or nitrogen cylinder; (10) thermostat.

double-walled glass tubular reactor (4) (length 340 mm, inner diameter 30 mm) and the irradiated aqueous solution (220 cm^3) was circulated (375 $cm^3\ min^{-1}$) continuously around the lamp, which was immersed directly in the solution. The phenol solution irradiated was thermostated at 25 °C. Oxygen or nitrogen gas was bubbled (855 $cm^3\ min^{-1}$) through the aqueous solution in the thermostated reservoir (6) and the solution was continuously stirred with a magnetic stirrer bar (7) during the experiments. Prior to each measurement, the gas was bubbled through the phenol solution at least for 10 min and the kinetic measurements were commenced by switching on the lamp.

The fluorimetric measurements were made with Hitachi F-2000 spectrofluorimeter. The excitation wavelength was 254 nm, and the intensity of the light emitted by the excited-state phenol molecules was determined at 298 nm.

The photolytic degradation of phenol was characterized by a linear fit to the decay curve of phenol, above 40% conversion ($0.999 > R^2 > 0.985$).

The concentrations of phenol and the various aromatic intermediates (1,2- and 1,4-dihydroxybenzene) were measured with an HPLC system, consisting of a Merck-Hitachi L-7100 low-pressure gradient pump equipped with a Merck-Hitachi L-4250 UV–vis detector ($\lambda = 210$ nm), applying a Lichrospher RP 18 column with a methanol/water (28/72) mixture as eluent. The organic acids formed during the irradiation were separated by using a GROM-RESIN ZH column and 10^{-2} mol dm^{-3} sulphuric acid as eluent in the same HPLC system ($\lambda = 206$ nm). The quantitative calibrations were carried out with standard solutions of known concentrations.

The sum of the hydrogen peroxide and alkylhydroperoxide concentrations was measured by the method of Zhang and Wong, which was modified by Gere et al. [18], using enzyme (horseradish peroxidase from Sigma) catalysed transformation of leuco crystal violet (Aldrich, Hungary) in tartrate buffer (pH 4.0). The absorbance of the solution was measured at 592 nm with a Hewlett-Packard (HP8452A) diode array spectrophotometer. The molar absorptivity of the crystal violet formed from the leuco crystal violet was 75 600 $mol^{-1}\ dm^3\ cm^{-1}$. The molar absorptivities of the investigated compounds (phenol, 1,2- and 1,4-dihydroxybenzene, 1,4-benzoquinone and oxalic acid) were determined by using the same spectrophotometer.

The LCMS measurements were carried out on an Agilent 1100 series LCMSD VL system consisting of a binary pump, a micro vacuum degasser, a diode array detector, a thermostated column compartment, a 1956A MSD and ChemStation data managing software. The chromatographic system was equipped with a Rheodyne Model 7725 injector with a 20 μl loop. The mass spectrometer was used in negative electrospray and atmospheric pressure ionization (ESI and APCI) modes. Ions in the range 50–700 *m/z* were registered in the conventional scanning mode.

The total organic carbon concentrations of the solutions investigated were measured by using a Euroglas 1200 TOC apparatus with 100 μl sample volumes.

3. Results and discussion

3.1. Effects of solvent and dissolved oxygen on the fluorescence of phenol

Excitation of phenol at 254 nm leads to the formation of its first excited state (1), which can decay by fluorescence. The fluorescence quantum yield and the lifetime of the excited state of phenol depend both on the nature of the solvent and on the presence of other compounds such as dissolved oxygen [6,19]. The excited state of aromatic compounds can be quenched by dissolved oxygen. Consequently, in the presence of oxygen, competition can occur between the decay of the excited state of phenol by fluorescence and its quenching by dissolved oxygen.

The fluorescence measurements were made both in oxygen-free and in oxygen saturated solutions in water and in acetonitrile as solvent. The wavelength of excitation was 254 nm. The results demonstrated that the intensity of the fluorescent light emitted at 298 nm was higher in oxygen-free acetonitrile than in aqueous solutions (Fig. 2). The concentration dependence of the intensity of the emitted light demonstrated that the relative contribution of internal quenching increased strongly with increase of the initial concentration of phenol in both cases (Fig. 2).

The dissolved oxygen had no effect on the intensity of the light emitted at 298 nm in water, whereas it strongly decreased the intensity in acetonitrile (Fig. 2). These results indicate that the quenching of the excited state of phenol due to collision with a dissolved oxygen molecule is not significant in water but in acetonitrile the dissolved oxygen plays a role as a physical quencher. A plausible explanation of these observations is the higher lifetime of excited phenol in acetonitrile than in water [6].

While the effective quenching of an excited phenol molecule by oxygen in acetonitrile can lead to $^1O_2$ (8) or $O_2^{\bullet-}$ (9), the rate of decomposition of phenol in water was found to be about three times higher than that in acetonitrile saturated with oxygen. In acetonitrile saturated with oxygen, the degradation of phenol was slower than in the oxygen-free solution, while dissolved

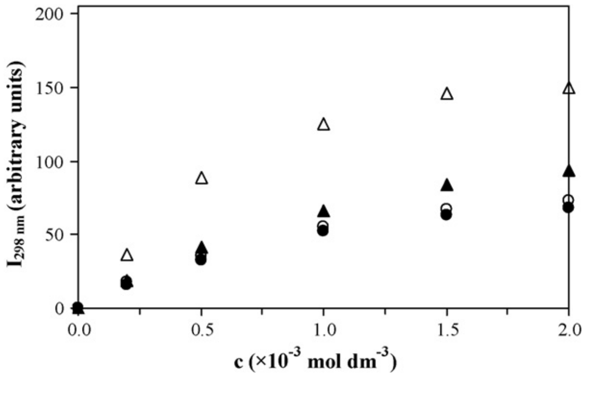

Fig. 2. Intensity of emitted fluorescence light detected at 298 nm during excitation of phenol at 254 nm in aqueous solution or in acetonitrile, as a function of the initial concentration of phenol. (○) Oxygen-free aqueous solution; (●) aqueous solution saturated with oxygen; (△) oxygen-free acetonitrile solution; (▲) acetonitrile solution saturated with oxygen.

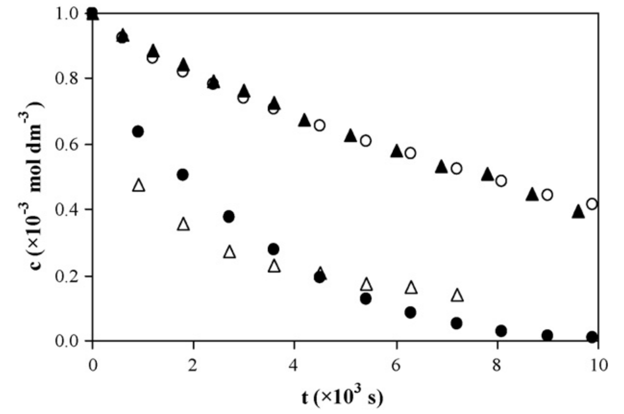

Fig. 3. Concentration of phenol in UV-irradiated aqueous or acetonitrile solution as a function of the duration of irradiation. (○) Oxygen-free aqueous solution; (●) aqueous solution saturated with oxygen; (△) oxygen-free acetonitrile solution; (▲) acetonitrile solution saturated with oxygen.

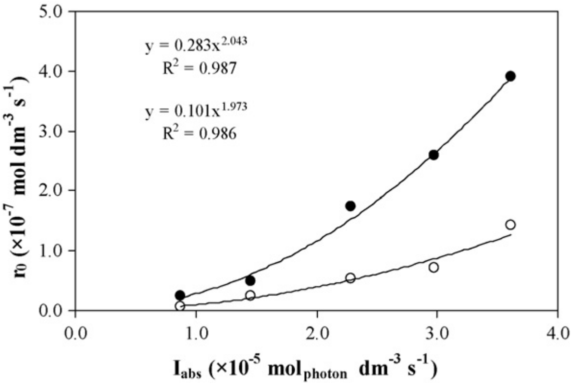

Fig. 4. Initial rate of degradation of phenol in aqueous solutions as a function of the photon flux of the 254 nm UV light at 1.0×10^{-3} M initial phenol concentration. (●) Solution saturated with oxygen; (○) oxygen-free solution.

oxygen enhanced the decomposition in water (Fig. 3). These experimental results demonstrated that dissolved oxygen has no effect via a direct reaction with the first excited state of phenol in aqueous solutions.

Another interesting observation was that, while mainly 1,2-dihydroxybenzene was formed as an aromatic intermediate in dissolved oxygen-containing aqueous solution, 1,4-dihydroxybenzene was detected in acetonitrile and 1,2-dihydroxybenzene was found only in traces. This observation is in accordance with the view that the reaction of phenol with singlet oxygen takes place by 1,4-cycloaddition [20], yielding 1,4-dihydroxybenzene.

3.2. Decomposition of phenol

In UV-irradiated solutions, the decomposition of phenol occurs by direct photolysis. The absorption of 254 nm UV light leads to the formation of excited-state phenol. Besides relaxation to the ground state, phenoxyl radical formation is expected [8,10]. Phenoxyl radical formation by direct photolysis is presumed to be a biphotonic, two-step process via the lowest excited state. The second photon is absorbed by the triplet state of the phenol molecule (6) and causes electron ejection. The radical cation formed has a very short lifetime in aqueous solutions; its deprotonation results in the phenoxyl radical. Both in oxygen-free and in solutions saturated with oxygen, the initial rate of degradation of phenol was found to be proportional to the square of the absorbed photon flux in UV-irradiated solutions (Fig. 4), which confirmed that the decomposition of phenol at 254 nm takes place via a biphotonic process.

The phenoxyl radical can exist as *ortho*-carbon, *para*-carbon or oxygen-centred resonance structures (10) that can also undergo self-reactions to form dimers [16]. The solubility of biphenols in water is rather low, but they can be dissolved in less polar solvents, such as acetonitrile. In nitrogen-saturated solutions, dimerization and polymerization of the phenoxyl radical were confirmed by HPLC-MS measurements. On the other hand, these solutions became turbid during irradiation; the turbidity disappeared after the addition of acetonitrile.

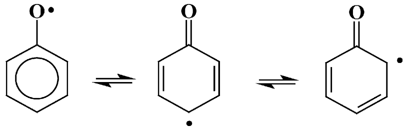

(10)

In the presence of dissolved oxygen the turbidity was not observed and the products of polymerization were not detected by HPLC-MS proving that dissolved oxygen inhibits the self-reactions of phenoxyl radicals. Phenoxyl-type radicals do not react with oxygen, despite having a considerable spin density on the carbon [16,21], but they can react with other radicals, such as $O_2^{\bullet-}$ ($k = 2 \times 10^9$ dm^3 mol^{-1} s^{-1} [22]) or $HO_2^\bullet$. The e_{aq}^- formed during the UV photolysis of phenol can be scavenged either by a proton (11) ($k = 2.3 \times 10^{10}$ dm^3 mol^{-1} s^{-1} [15]) or by dissolved oxygen (12) ($k = 1.9 \times 10^{10}$ dm^3 mol^{-1} s^{-1} [14]). Both of them can result finally in $HO_2^\bullet$:

$$H^+ + e_{aq}^- \rightarrow H^\bullet \xrightarrow{O_2} HO_2^\bullet \tag{11}$$

$$O_2 + e_{aq}^- \rightarrow O_2^{\bullet-} \underset{-H^+}{\overset{H^+}{\rightleftarrows}} HO_2^\bullet \tag{12}$$

Bussandri and von Willigen [8] demonstrated that the phenoxyl radical concentration is independent of pH in the range 7–2, but the concentration of the e_{aq}^- is strongly attenuated on the decrease of pH, which is attributed to scavenging of the e_{aq}^- by protons (11).

In UV-irradiated solutions saturated with oxygen, about 30% of the decomposed phenol was present as dihydroxybenzene (1,2- and 1,4-dihydroxybenzene) (Fig. 5b). Although the UV photolysis of aromatic compounds has been investigated in several publications, knowledge of the formation of dihydroxybenzenes from the phenoxyl radical is not complete. The theoretical calculations of Skokov et al. [23] demonstrated that their formation is possible via the reaction of $HO_2^\bullet$ with the phenoxyl radical (13) and (14). The recombination of the phenoxyl radical with $HO_2^\bullet$ leads to stable phenoxyl–OOH adducts, formed via barrierless addition of $HO_2^\bullet$ in the ortho and para positions, respectively. The further transformation of phenoxyl-OOH finally yields to dihydroxybenzenes through the simultaneous shift of two H atoms (13). In the next step, a H atom

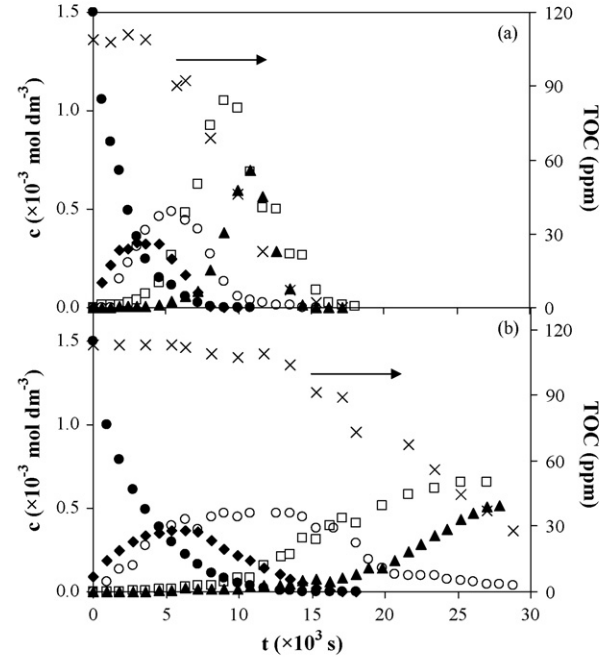

Fig. 5. Time dependences of concentrations of phenol (●), the overall concentrations of 1,2- and 1,4-dihydroxybenzene (◆), the overall concentrations of malic, maleic and tartaric acids (○); concentrations of oxalic acid (▲), the overall concentrations of the hydroperoxide (□) and total organic carbon (TOC) concentrations (×) in (a) UV/VUV and (b) UV-irradiated solutions saturated with oxygen at 1.5×10^{-3} mol dm^{-3} initial concentration.

from the OH group and an OH fragment from the OOH group form a water molecule as product.

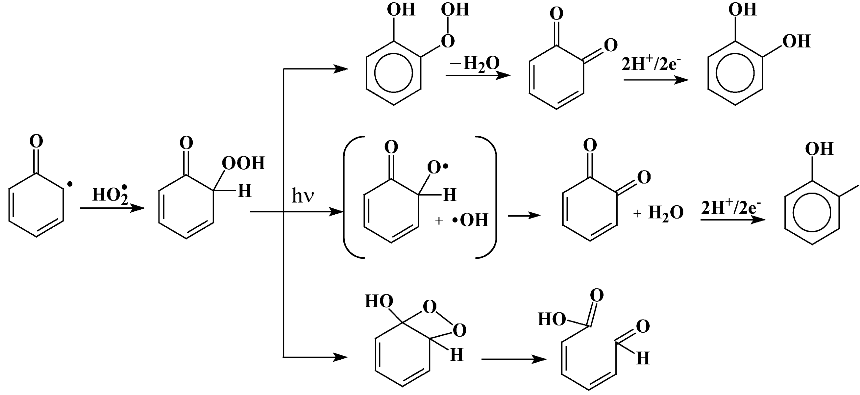

(13)

(14)

(15)

On the other hand, the phenoxyl–OOH formed can also decompose via photolysis. The semiquinone radical obtained is an efficient H donor and can scavenge HO$^\bullet$ in either a simultaneous cage or a subsequent fast reaction (14). Another possible pathway for the transformation of phenoxyl–OOH can lead to the opening of the aromatic ring via attack on a neighbouring carbon atom by an O atom of the OOH group (15). In UV-irradiated solutions saturated with oxygen, in parallel with the decomposition of phenol and the formation of dihydroxybenzenes, the aliphatic intermediates resulted in ring-opening reactions (Fig. 5b). About 25–30% of the decomposed phenol was detected as the sum of maleic, malic and tartaric acids at 1.5×10^{-3} mol dm^{-3} initial concentration.

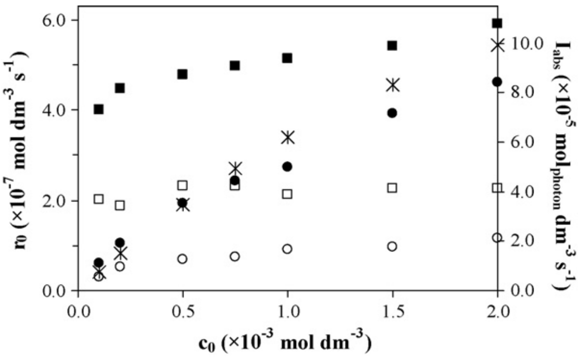

Fig. 6. Photon flux absorbed by phenol at 254 nm (*), calculated according to the Beer–Lambert law ($\varepsilon_{\text{phenol}}(254\,\text{nm}) = 516$ mol^{-1} dm^3 cm^{-1}; $l = 0.475$ cm) and initial rate of degradation of phenol as a function of the initial concentration in: UV/VUV-irradiated solutions saturated with oxygen (■); UV/VUV-irradiated oxygen-free solutions (□); UV-irradiated solutions saturated with oxygen (●); UV-irradiated oxygen-free solutions (○).

In UV/VUV-irradiated solutions, the decomposition of phenol can take place either by direct photolysis at 254 nm or by HO$^\bullet$-based reactions. The HO$^\bullet$ originates from water by homolytic dissociation caused by 185 nm light. The degradation of aromatic compounds in water by HO$^\bullet$ yields dihydroxycyclohexadienyl (DHCHD) radicals via the addition of HO$^\bullet$ to the aromatic ring ($k = 1.8 \times 10^{10}$ dm^3 mol^{-1} s^{-1} [24]) to the *ortho* or *para* position of the OH functional group of phenol [16]. Naturally, H$^\bullet$ can also add to the aromatic ring ($k = 1.7 \times 10^9$ dm^3 mol^{-1} s^{-1} [15]), resulting in hydroxycyclohexadienyl (HCHD) radicals. The further transformations of DHCHD and HCHD radicals depend strongly on the concentration of dissolved oxygen. In solutions saturated with oxygen, the addition of dissolved oxygen to these carbon-centred radicals ($k(\text{HCHD} + \text{O}_2) = 3.1 \times 10^8$ dm^3 mol^{-1} s^{-1} [25]) predominates, and yields peroxyl radicals. The further transformations of the DHCHD-peroxyl radicals result in dihydroxybenzenes by HO$_2^\bullet$ elimination (16), while the same elimination from the HCHD-peroxyl radical yields phenol (18). In UV/VUV-irradiated solutions saturated with oxygen, the 30% decomposed phenol was present as the sum of 1,2- and 1,4-dihydroxybenzene similarly as for UV-irradiated solutions (Fig. 5). On the other hand, in the series of HCHD and DHCHD radicals, competition occurs between $HO_2^{\bullet}$ elimination and fragmentation of the ring; this can be attributed to intramolecular addition of a peroxyl radical function to a diene double bond (17) and (19). The opening of the aromatic ring was confirmed by the fact that, besides dihydroxybenzenes, the formation of aliphatic carboxyl acids (maleic, malic and tartaric acids) was observed in parallel with the decomposition of phenol and the formation of aromatic intermediates (Fig. 5a).

The $HO_2^{\bullet}$ resulting either from the addition of an oxygen molecule to $H^{\bullet}$ (11) or from elimination from organic peroxyl radicals (16) and (18) can also play an important role in the degradation of phenol. For example, $HO_2^{\bullet}$ can add to phenol (20). The subsequent reaction with molecular oxygen and elimination of $HO_2^{\bullet}$ finally leads to the formation of an open-chain product [26]:

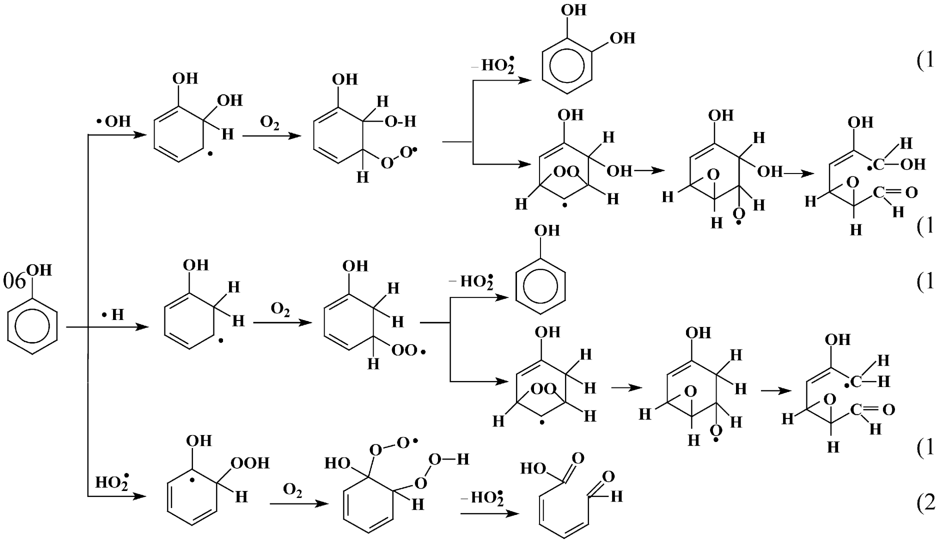

(16)

(17)

(18)

(19)

(20)

The initial rate of degradation of phenol was found to be systematically higher in the UV/VUV than in the UV-irradiated solutions regardless of whether they were oxygen-saturated or oxygen-free (Fig. 6). This is most likely due to the contribution of $HO^{\bullet}$-based reactions to the decomposition of phenol caused by the presence of VUV light. Thus, in UV/VUV-irradiated solutions the degradation of phenol takes place by both direct photolysis at 254 nm and $HO^{\bullet}$-based reactions while in UV-irradiated ones the decomposition of phenol is initiated only by direct photolysis at 254 nm.

The relative contributions of the direct photolysis by 254 nm light and $HO^{\bullet}$-based reactions to the degradation of phenol should depend on the amount of light absorbed at different wavelengths by the irradiated solution. The VUV light is fully absorbed by water in a 0.1 mm thick layer [13] and therefore $HO^{\bullet}$ is formed at a stationary rate. On the other hand, the amount of light absorbed at 254 nm depends on the phenol concentration according to the Lambert–Beer correlation. Thus, while the $HO^{\bullet}$ concentration is independent of the initial concentration of phenol, the concentration of the phenoxyl radical should increase with increase of the phenol concentration.

The rates of degradation of phenol slightly increased with the initial concentration when the UV/VUV lamp was applied, and exceeded the corresponding values measured in UV-irradiated solutions mainly at lower initial concentrations (Fig. 6). At the same time, when the UV lamp was used the initial rate of degradation dramatically increased on increase of the initial phenol concentration, mainly in the solutions saturated with oxygen (Fig. 6). Consequently, the difference between the degradation rates in UV- and UV/VUV-irradiated solutions decreased strongly with increase of the initial phenol concentration, in both oxygen-saturated and oxygen-free solutions (Fig. 6).

These results allow the supposition that the initial step of phenol transformation in UV/VUV-irradiated solutions at lower phenol initial concentrations proceeds mainly via $HO^{\bullet}$-based reactions. Nevertheless, it must be borne in mind that, besides the $HO^{\bullet}$-based reactions, the relative contribution of the direct photolysis of phenol at 254 nm should increase with increase of the initial phenol concentration in UV/VUV-irradiated solutions, similarly as in UV-irradiated solutions, and this seems to be the predominant pathway at higher initial phenol concentrations.

Phenol decomposes more slowly under oxygen-free conditions than in solutions saturated with oxygen (Fig. 6). For UV/VUV irradiation, the concentration of $HO^{\bullet}$ at a given light intensity depends strongly on the concentration of dissolved oxygen [27]. The dissolved oxygen inhibits the recombination of $H^{\bullet}$ and $HO^{\bullet}$ ($k = 7 \times 10^{9}\ \mathrm{dm^3\,mol^{-1}\,s^{-1}}$ [28]) originating from water due to the addition of O_2 to $H^{\bullet}$. Thus, the dissolved oxygen causes higher concentrations both of $HO^{\bullet}$ and $HO_2^{\bullet}$ and a lower concentration of $H^{\bullet}$. Consequently, in UV/VUV-irradiated solutions saturated with oxygen, the decomposition of phenol is most probably initiated by $HO^{\bullet}$ or $HO_2^{\bullet}$ and, in parallel with this the role of $H^{\bullet}$ becomes negligible. On the other hand, as for the possible pathways for the decomposition of phenol demonstrated above, the dissolved oxygen opens up a new pathway for the formation of $HO_2^{\bullet}$, partly via the peroxyl radical, in both UV- and UV/VUV-irradiated solutions.

3.3. Effects of methanol as $^{\bullet}OH$ scavenger

As described above, in UV/VUV-irradiated aqueous solutions the formation of $HO^{\bullet}$ is expected and is probably

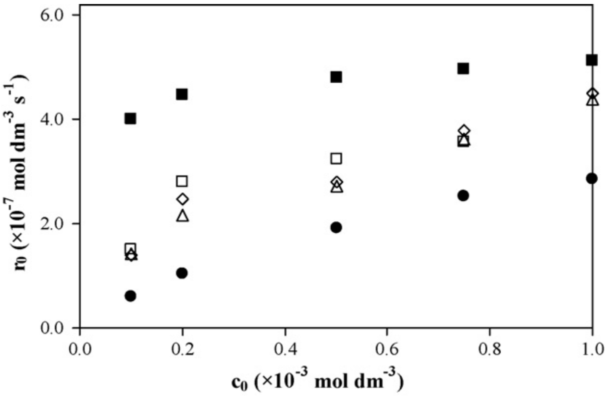

Fig. 7. Effects of methanol as $^\bullet$OH radical scavenger on initial rate of degradation of phenol as a function of initial concentration of phenol in UV/VUV-irradiated solutions saturated with oxygen. (■) UV/VUV-irradiated solution without methanol; (●) UV-irradiated solutions without methanol; (□) UV/VUV-irradiated solutions with 10^{-2} mol dm^{-3} methanol; (◊) UV/VUV-irradiated solution with 10^{-1} mol dm^{-3} methanol; (△) UV/VUV-irradiated solution with 1.0 mol dm^{-3} methanol.

responsible for the higher rate of degradation of phenol in UV/VUV than in UV-irradiated solutions. Methanol was used as HO$^\bullet$ scavenger [13,15]:

$$\mathrm{CH_3OH + HO^\bullet \rightarrow {}^\bullet CH_2OH + H_2O}, \quad k = (0.78\text{–}1.0)\times 10^9\ \mathrm{dm^3\,mol^{-1}\,s^{-1}} \tag{21}$$

in order to study the role and the relative contribution of HO$^\bullet$-based reactions to the decomposition of phenol in UV/VUV-irradiated solutions. Experiments were performed in the initial phenol concentration range (0.1–1.0) × 10^{-3} mol dm^{-3} (Fig. 7).

The inhibitory effect of methanol was found to depend strongly on the initial concentration of phenol. Its addition inhibited the degradation of phenol at lower initial concentrations, but this inhibitory effect became negligible at a phenol concentration 1.0×10^{-3} mol dm^{-3} even at a concentration of methanol 1.0 mol dm^{-3} (Fig. 7). This dependence of the inhibitory effect of methanol on the initial phenol concentration confirmed that the relative contribution of HO$^\bullet$-based reactions to the degradation of phenol decreased with increasing initial phenol concentration in UV/VUV-irradiated solutions.

As expected, the addition of methanol did not have an appreciable effect on the rate of degradation of phenol in UV-irradiated solutions, when the phenol decomposition is initiated by direct photolysis. However, it should be noted that, although methanol addition inhibited the degradation of phenol in UV/VUV-irradiated solutions, decomposition was found to be slower in UV-irradiated solutions than in methanol-containing UV/VUV-irradiated ones, even at 1.0 mol dm^{-3} methanol (Fig. 7). One plausible explanation of this is that the HO$^\bullet$-initiated decomposition of methanol is the concomitant of HO$_2^\bullet$ formation (23) in solutions saturated with oxygen [29]:

$$\mathrm{{}^\bullet CH_2OH + O_2 \rightarrow {}^\bullet OOCH_2OH}, \quad k = 4.2\times 10^9\ \mathrm{dm^3\,mol^{-1}\,s^{-1}} \tag{22}$$

$$\mathrm{{}^\bullet OOCH_2OH \rightarrow CH_2O + HO_2^\bullet}, \quad k = 5.0\times 10^2\ \mathrm{s^{-1}} \tag{23}$$

Thus, the HO$_2^\bullet$ concentration is likely to be higher in the methanol-containing UV/VUV-irradiated system as compared with UV-irradiated solutions at the same initial concentration of phenol.

The inhibitory effect of methanol was more marked in solutions saturated with oxygen than in oxygen-free ones. Addition of methanol to phenol in an initial concentration of 1.0×10^{-4} mol dm^{-3}, solution saturated with oxygen decreased its initial rate of degradation by 60–70%, while the decrease in the oxygen-free solution was only 20%. A plausible explanation of this is the higher HO$^\bullet$ concentration due to the presence of dissolved oxygen.

It should be noted that the effect of methanol on the conversion of the dihydroxybenzenes formed is not considerable in UV/VUV-irradiated solutions, although their rates of formation and decomposition do decrease, depending on the initial concentration of phenol, similarly to the degradation.

3.4. *Aromatic intermediates*

1,2- and 1,4-dihydroxybenzene were measured as aromatic intermediates in both the UV- and the UV/VUV-irradiated phenol solutions saturated with oxygen. Their formation might be initiated either from phenol by HO$^\bullet$-based reaction (16) or via the reaction of HO$_2^\bullet$ with the phenoxyl radical (13) and (14) originating from direct photolysis at 254 nm. The formation of dihydroxybenzenes from the peroxyl radical is presumed to occur through the formation of benzoquinone (13) and (14), but benzoquinone was found in the irradiated solutions only in traces. The reason for this may be that its decomposition is very fast during 254 nm irradiation either in oxygen-saturated or in oxygen-free solutions (Fig. 8), most probably because of the high molar absorption coefficient of 1,4-benzoquinone ($\varepsilon_{254\,\mathrm{nm}}$ = 9 000 mol^{-1} dm^3 cm^{-1}).

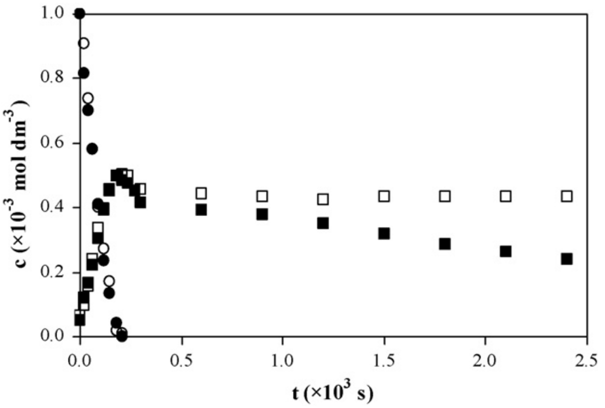

Fig. 8. Concentration of 1,4-benzoquinone and 1,4-dihydroxybenzene formed in UV-irradiated 1,4-benzoquinone solutions at 1.0×10^{-3} mol dm^{-3} initial concentration. (●) Concentration of 1,4-benzoquinone in solution saturated with oxygen; (○) concentration of 1,4-benzoquinone in oxygen-free solution; (■) concentration of 1,4-dihydroxybenzene in solution saturated with oxygen; (□) concentration of 1,4-dihydroxybenzene in oxygen-free solution.

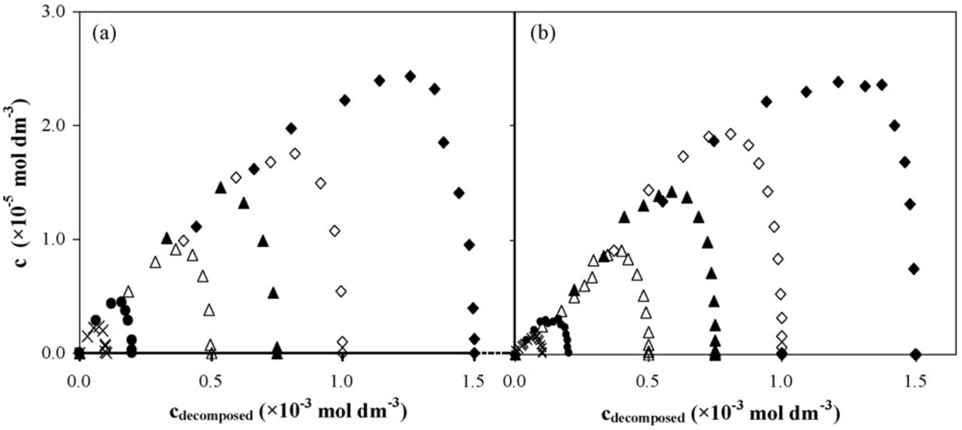

Fig. 9. The overall concentrations of 1,2- and 1,4-dihydroxybenzene as a function of concentration of decomposed phenol in (a) UV/VUV and (b) UV-irradiated solutions at different initial concentrations. (×) 1.0×10^{-4} mol dm^{-3}; (●) 2.0×10^{-4} mol dm^{-3}; (△) 5.0×10^{-4} mol dm^{-3}; (▲) 7.5×10^{-4} mol dm^{-3}; (◇) 1.0×10^{-3} mol dm^{-3}; (◆) 1.5×10^{-3} mol dm^{-3} in solutions saturated with oxygen.

1,4-Benzoquinone (1.0×10^{-3} mol dm^{-3}) decomposes within 5 min in UV-irradiated solution and half of the decomposed amount was detected as 1,4-dihydroxybenzene (Fig. 8).

In all cases, the concentration of 1,2-dihydroxybenzene exceeded that of 1,4-dihydroxybenzene. About 30% of the decomposed phenol was present as the sum of dihydroxybenzenes both in UV (23% 1,2-dihydroxybenzene and 7% 1,4-dihydroxybenzene) and in UV/VUV (26% 1,2-dihydroxybenzene and 4% 1,4-dihydroxybenzene)-irradiated solutions (Fig. 9). In the absence of VUV photons, the rates of accumulation and degradation of both aromatic intermediates were found to be considerably lower than in their presence (Fig. 5), but the sum of their concentrations as a function of the concentration of decomposed phenol exhibits the same dependence (Fig. 9). The formation of these aromatic intermediates starts together with the decomposition of phenol and they are present in the irradiated solution until the complete decomposition of phenol (Fig. 5).

Naturally, the dihydroxybenzenes can undergo similar reactions to those of phenol. Both detected aromatic intermediates react with HO$^\bullet$ (k(1,4-dihydroxybenzene + HO$^\bullet$) = 2.1×10^{10} dm^3 mol^{-1} s^{-1} [24]) and k(1,2-dihydroxybenzene + HO$^\bullet$) = 1.1×10^{10} dm^3 mol^{-1} s^{-1}) and absorb at 254 nm ($\varepsilon_{254\,\mathrm{nm}}$(1,2-dihydroxybenzene) ≈ 370 mol^{-1} dm^3 cm^{-1} and $\varepsilon_{254\,\mathrm{nm}}$(1,4-dihydroxybenzene) ≈ 70 mol^{-1} dm^3 cm^{-1}).

The decompositions of these aromatic intermediates were investigated and compared in UV- and UV/VUV-irradiated solutions at 5.0×10^{-4} mol dm^{-3} initial concentrations (Fig. 10).

The presence of 185 nm VUV light caused much faster decomposition for all of the investigated aromatic intermediates, similarly as for phenol. In UV-irradiated solution saturated with oxygen, the decomposition of 1,4-dihydroxybenzene was found to be faster than that of 1,2-dihydroxybenzene (Fig. 10b), despite the fact that the molar absorption coefficient at 254 nm is much higher for 1,2-dihydroxybenzene. At the same time, the rate of degradation of these aromatic substances changed according to their molar absorption coefficients in UV-irradiated oxygen-free solutions (Fig. 10d). However, it should be noted that the rate of direct photooxidation depends strongly not only on the molar absorptivity, but also on the quantum yields of the decompositions of these aromatic substances and dissolved oxygen can strongly effect the pathway for the decomposition.

3.5. Aliphatic intermediates and total organic carbon concentration

The total organic carbon contents, the overall concentration of aliphatic acids and the overall concentration of organic hydroperoxides (methyl and ethyl hydroperoxides) were measured during the decomposition of phenol at an initial concentration of 1.5×10^{-3} mol dm^{-3} both in UV- and UV/VUV-irradiated aqueous solutions saturated with oxygen (Fig. 5). The same aliphatic intermediates, e.g. maleic, malic, tartaric and oxalic acids, were identified in UV- and UV/VUV-irradiated solutions saturated with oxygen. Maleic, malic and tartaric acids were formed in parallel with the decomposition of phenol. At the same time, the accumulation of oxalic acid and organic hydroperoxides became considerable when the phenol, dihydroxybenzenes and longer-chain carboxylic acids (maleic, malic and tartaric acids) disappeared from the solution (Fig. 5), which suggests that the fragmentation becomes significant only after the disappearance of aromatic compounds.

The accumulation and decomposition of oxalic acid and hydroperoxides were much faster in the UV/VUV-irradiated solutions than in the UV-irradiated solutions (Fig. 5). Thus, it can be stated that 185 nm light, in spite of its relatively low intensity, not only causes a considerably higher rate of degradation of phenol, but also plays an important role in the fragmentation and hence the complete oxidation of the intermediates formed. The concentration of hydroperoxides demonstrated maximum curves both during UV and UV/VUV light irradiation; the maximum values were much higher for the UV/VUV than for the UV-irradiated solutions (Fig. 5). The very similar time dependences of the oxalic acid and hydroperoxide concentrations suggest that hydroperoxides are important and readily decomposable intermediates in the oxidation process. They can form

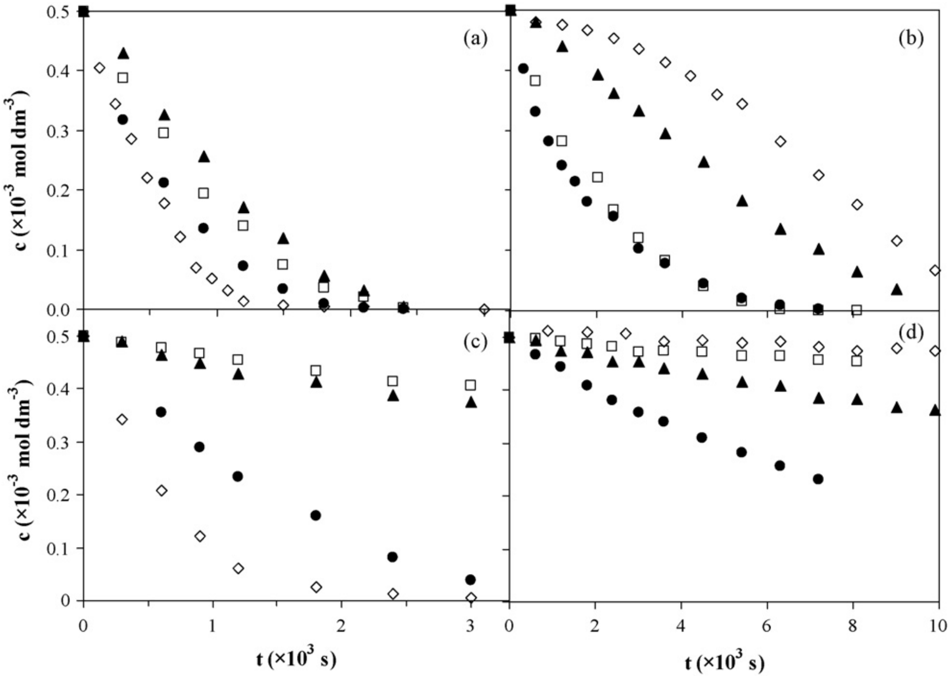

Fig. 10. Concentrations of phenol (●), 1,4-dihydroxybenzene (□), 1,2-dihydroxybenzene (▲) and oxalic acid (◊) as a function of the duration of irradiation in: (a) UV/VUV-irradiated solution, saturated with oxygen, (b) UV-irradiated solution saturated with oxygen, (c) UV/VUV-irradiated, oxygen-free solution, and (d) UV-irradiated, oxygen-free solution at 5.0×10^{-4} mol dm^{-3} initial concentrations.

via addition of the $HO_2^{\bullet}$ radical to the other carbon-centred radicals (23) or via H abstraction by peroxyl radicals (24):

$$R^{\bullet} + HO_2^{\bullet} \rightarrow ROOH \quad (23)$$

$$ROO^{\bullet} + RH \rightarrow ROOH + R^{\bullet} \quad (24)$$

Among the determined aliphatic intermediates the concentration of oxalic acid was highest. Accordingly, we considered that investigation of its decomposition by UV and UV/VUV light can furnish useful information on the degradation of the aliphatic intermediates. The molar absorption of oxalic acid at 254 nm is rather low (50 mol^{-1} dm^{3} cm^{-1} [30]). In oxygen-free solution, the decomposition of oxalic acid under UV-irradiation was negligible (Fig. 10d), while the degradation began with an induction period in solution saturated with oxygen (Fig. 10b). This suggests that the reactive species (probably oxygen containing radicals) formed during the decomposition and further transformation of oxalic acid played important roles and accelerated the degradation. At the same time, in UV/VUV-irradiated solutions the decomposition of oxalic acid took place without an induction period (Fig. 10a and c) and was about one magnitude faster as compared with that on UV irradiation.

A significant difference was found between the formation of hydroperoxides in UV- and UV/VUV-irradiated oxalic acid solutions saturated with oxygen. The accumulation of hydroperoxide started sharply and immediately after the UV/VUV lamp was switched on. At the same time, the concentration of hydroperoxide increased slowly in the UV-irradiated solutions. The concentration of hydroperoxide exhibited maximum curves in both cases, but the maximum value was five times higher for the UV/VUV than for the UV-irradiated solutions.

During photodegradation, the irradiated solution had a minimum pH of 3.2–3.5. This trend reflects the phenol decomposition path during UV or UV/VUV irradiation: phenol → (aromatic intermediates) → acid intermediates → $CO_2\uparrow + H_2O$. It is very important that the rate of total mineralization of phenol is much higher when a UV/VUV lamp is used, as demonstrated by the change in the total organic carbon content (Fig. 5).

4. Conclusions

The photolysis of phenol was investigated and compared in aqueous solutions irradiated with either UV or UV/VUV lamp. In UV-irradiated solutions, the decomposition of phenol is initiated by direct photolysis via a biphotonic process, while in UV/VUV-irradiated solutions the decomposition of phenol can also take place by $HO^{\bullet}$-based reactions. The results demonstrated that the VUV light plays an important role not only in the faster decomposition of phenol, but also in the opening of the aromatic ring, the fragmentation and decomposition of the intermediates and finally the total oxidation of phenol, although its intensity is rather low as compared with the intensity of 254 nm light.

The relative contributions of $HO^{\bullet}$-based reactions and direct photolysis in UV/VUV-irradiated solutions were found to depend strongly on the initial phenol concentration. At lower initial phenol concentrations the $HO^{\bullet}$-based reactions seem to predominate when a UV/VUV lamp is used, but at higher phenol initial concentrations it decomposed mainly by direct photolysis at 254 nm. This was confirmed by investigation of the inhibitory effect of methanol as $HO^{\bullet}$ scavenger.

Dissolved oxygen strongly increased the rate of degradation of phenol and its intermediates, probably because of the formation of oxygen-containing reactive species such as organic peroxyl radicals, $HO_2^{\bullet}/O_2^{\bullet-}$, whose relative contribution to the decomposition increases together with increase of the initial concentration of phenol. Additionally, dissolved oxygen caused higher $HO^{\bullet}$ concentration in the presence of VUV light.

The decompositions of aromatic intermediates and of oxalic acid as aliphatic intermediate were also investigated. The results demonstrated that, in UV-irradiated, oxygen-free solutions the rates of degradation of the investigated substances were determined by the molar absorption coefficients. However, in UV-irradiated solution saturated with oxygen, the decomposition of 1,4-dihydroxybenzene was found to be faster than that of 1,2-dihydroxybenzene and the degradation of oxalic acid began with an induction period. The presence of 185 nm VUV light strongly accelerated the decomposition of each investigated substance.

Acknowledgements

This work was financially supported by grants from the National Science Foundation of Hungary (OTKA T/04355 and T/15 043273) and the Hungarian National Office of Research and Technology (NKFP 3A/089/2004 RET-07/2005 and GVOP 3.1.1.-2004-05-0259/3.0). The assistance of LightTech (Lajos Reich and László Benkő) is also highly appreciated.

References

[1] O. Legrini, E. Oliveros, A.M. Braun, Chem. Rev. 93 (1993) 671.

[2] W.J. Masschelein, Ultraviolet Light in Water and Wastewater Sanitation, Lewis Publishers, 2002, pp. 13–22.

[3] M.I. Stephan, WilliamsonF C.T., in: S. Parsons (Ed.), Advanced Oxidation Processes for Water and Wastewater Treatment, IWA Publishing, Cornwall, UK, 2004, pp. 49–80.

[4] J. Audureau, C. Filiol, P. Boule, J. Lemaire, J. Chim. Phys. 73 (1976) 513.

[5] D. Hayashi, W. Hoeben, G. Dooms, E. von Veldhuizen, W. Rutgers, G. Kroesen, Appl. Optics 40 (2001) 986.

[6] R. Hermann, G.R. Mahalaxmi, T. Jochum, T. Naumov, O. Brede, J. Phys. Chem. A: Chem. 106 (2002) 2379.

[7] G. Siuzdak, S. North, J.J. BelBruno, J. Phys. Chem. 95 (1991) 5186.

[8] A. Bussandri, H. von Willigen, J. Phys. Chem. A: Chem. 106 (2002) 1524.

[9] J. Jortner, M. Ottolenghi, G. Stein, J. Am. Chem. Soc. 85 (1963) 2712.

[10] H.-I. Joschek, S.I. Miller, J. Am. Chem. Soc. 88 (1966) 3273.

[11] J. Feitelson, E. Hayon, A. Treinin, J. Am. Chem. Soc. 95 (1973) 1025.

[12] T.A. Gadosy, D. Shukla, L.J. Johnston, J. Phys. Chem. 103 (1999) 8834.

[13] M.G. Gonzalez, E. Oliveros, M. Wörner, A.M. Braun, J. Photochem. Photobiol. A: Chem. 5 (2004) 225.

[14] A.J. Elliot, Radiat. Phys. Chem. 34 (1989) 753.

[15] G.V. Buxton, C.L. Greenstock, W.P. Helman, A.B. Ross, J. Phys. Chem. Ref. Data 17 (1988) 513.

[16] C.V. Sonntag, H.-P. Schuchmann, in: Z.B. Alfassi (Ed.), The Chemistry of Free Radicals: Peroxyl Radicals, John Wiley Sons, Chichester, England, 1997, p. 172.

[17] C.G. Hatchard, C.A. Parker, Proc. Roy. Soc. A 235 (1956) 518.

[18] E. Gere, B. Bérczi, P. Simándi, G. Wittmann, A. Dombi, Int. J. Environ. Anal. Chem. 82 (2002) 443.

[19] D.V. Bent, E. Hayon, J. Am. Chem. Soc. 97 (1974) 2606.

[20] D. Madhavan, K. Pitchumani, J. Photochem. Photobiol. A: Chem. 153 (2002) 205.

[21] E.P. Hunter, M.F. Desrosiers, M.G. Simic, Free Radic. Biol. Med. 6 (1989) 581.

[22] M. Jonsson, J. Lind, T. Reitberger, T.E. Eriksen, G. Merényi, J. Phys. Chem. 97 (1993) 8229.

[23] S. Skokov, A. Kazakov, F.L. Dryer, Proceedings of the 4th Joint Meeting of the U.S. Sections of the Combustion Institute, Drexel University, Philadelphia, 2005.

[24] G.E. Adams, J.W. Boag, J. Currant, B.D. Michael, in: M. Elbert, J.P. Keene, A.J. Swallow, J.H. Baxendale (Eds.), Pulse Radiolysis, Academic Press, New York, 1965, p. 131.

[25] X.M. Pan, C.V. Sonntag, Z. Naturforsch. B45 (1990) 1337.

[26] N. Getoff, Radiat. Phys. Chem. 47 (1996) 581.

[27] Zs. László, A. Dombi, Chemosphere 46 (2002) 491.

[28] J.K. Thomas, Trans. Faraday Soc. 61 (1965) 702.

[29] J. Rabani, D. Klung-Roth, J. Phys. Chem. 78 (1974) 2089.

[30] N.V. Leitner, M. Doré, Water Res. 31 (1997) 1383.